Article

# HRP-Mimicking DNAzyme-Catalyzed in Situ Generation of Polyaniline to Assist Signal Amplification for Ultrasensitive Surface Plasmon Resonance Biosensing

Haiyin Li, Jiafu Chang, Ting Hou, and Feng Li

*Anal. Chem.*, **Just Accepted Manuscript** • DOI: 10.1021/acs.analchem.6b02988 • Publication Date (Web): 08 Dec 2016

# HRP-Mimicking DNAzyme-Catalyzed *in Situ* Generation of Polyaniline to Assist Signal Amplification for Ultrasensitive Surface Plasmon Resonance Biosensing

Haiyin Li,[§] Jiafu Chang,[§] Ting Hou, and Feng Li*

College of Chemistry and Pharmaceutical Sciences, Qingdao Agricultural University, Qingdao 266109, People's Republic of China

[§] H. Y. Li and J. F. Chang contributed equally to this work.

* Corresponding author. Tel/Fax: 86-532-86080855; E-mail: lifeng@qust.edu.cn

## ABSTRACT

As is well known, the horseradish peroxidase (HRP)-mimicking DNAzyme, i.e. hemin/G-quadruplex, can effectively catalyze the polymerization of aniline to form DNA-guided polyaniline. Meanwhile, polyaniline exhibits extraordinary electrical, electrochemical and redox properties, as well as excellent SPR signal enhancing ability. Herein, we report a novel ultrasensitive surface plasmon resonance (SPR) biosensor based on HRP-mimicking DNAzyme-catalyzed *in situ* formation of polyaniline for signal amplification, using bleomycin (BLM) as the proof-of-concept analyte. The recognition and the subsequent cleavage of DNA probe P1 by BLM switches off the hybridization between P1 and the G-rich DNA probe P2, resulting in less hemin/G-quadruplex complexes and reduced DNA-guided polyaniline deposition on SPR Au disk surface. As compared to the case that BLM is absent, significant SPR angle shift is observed, which is dependent on BLM concentration. Therefore, ultrasensitive SPR detection of target BLM is realized, with a detection limit down to 0.35 pM, much lower than those reported in literature. Moreover, the as-proposed SPR biosensor has been successfully applied for the detection of BLM spiked in human serum samples. The HRP-mimicking DNAzyme-catalyzed *in situ* polyaniline deposition and polyaniline-assisted signal amplification not only significantly improves the specificity and the sensitivity of BLM assay, but also allows the ultrasensitive detection of other biomolecules by simply changing the specific target recognition DNA sequences, thus providing a versatile SPR biosensing platform for ultrasensitive detection of a variety of analytes, and showing great potential to be applied in the fields of bioanalysis and clinical biomedicine.

## INTRODUCTION

The simple, sensitive and selective detection of target biomolecules has become a primary and hot research topic in a variety of fields including molecular diagnosis, environmental monitoring, food safety, agricultural industry, *etc*.[1,2] Over the past decade, various biosensors, such as electrochemistry,[3] fluorescence,[4] photoelectrochemistry,[5] chemiluminescence,[6] and electro-chemiluminescence[7] have been developed as alternative strategies to conventional sensing methods for various analyte detections. In this regard, surface plasmon resonance (SPR) biosensing shows great promise as a powerful analytical tool due to its noticeable advantages of good reliability, high sensitivity, multiplexed detection, etc.[8-13] Up to now, a large number of modern SPR assays adopted external labels with high refractive index, which enhances the performance of these SPR biosensors. In most of the aforementioned methods, signal amplification relied on a secondary hybridization of the sensing probes to the DNA immobilized on the SPR surface.[14-16] But an unsuitable signal amplification strategy to immobilize high refractive material-labeled DNA on SPR Au surface may result in no or inaccurate signal response. At the same time, the secondary hybridization strategy for enhancing SPR response is rather tedious and difficult to directly immobilize external labels on Au surface, limiting the routine use of SPR biosensors, and thus it is difficult to realize simple, reliable, ultrasensitive and multiplexed SPR assays. Meanwhile the DNA coverage on Au surface and the labeling of DNA probes may introduce additional complications. Therefore, it is desirable to design a facile and efficient signal amplification strategy for ultrasensitive SPR detection by eliminating the need of a secondary hybridization process.

Polyaniline, an important member of the conducting polymer family, has attracted increasing fundamental and practical research interest in chemo/biosensors,[17-19] due to its extraordinary electrical, electrochemical and redox properties, as well as good environmental characteristics.[20,21] For instance, Cai's

group reported a glucose detection strategy based on direct electron transfer reaction of glucose oxidase immobilized on highly ordered polyaniline nanotubes.[19] Apte's group reported a highly sensitive polyaniline-based microbial biosensor for selective detection of lindane.[22] In addition, polyaniline nanomaterials exhibited a SPR effect during the photo-catalytic or SPR process, which can substantially increase the light absorption, and thus improve the photo-catalytic or SPR performance.[23-25] Therefore, incorporating polyaniline nanomaterials into DNA structures immobilized on Au disk surface can effectively enhance the SPR conversion efficiency and improve the detection sensitivity. Until now, polyaniline-assisted sensing strategies have been mainly applied in electrochemical assays,[26,27] and one of the few approaches for SPR sensing relied on the horseradish peroxidase (HRP) catalyzed polyaniline formation for signal amplification.[28] However, some major shortcomings, such as high cost, easy loss of catalytic activity and strict experimental conditions, limit the further application of HRP in polyaniline formation. Thus, it is desirable to develop novel strategies for constructing convenient, efficient and versatile signal output/amplification systems based on polyaniline for ultrasensitive SPR detection.

In the past few years, DNAzymes have been frequently applied in various biosensors ascribing to their relatively easy preparation, low cost, and good stability.[29,30] One of the most explored DNAzymes for bioanalysis is the horseradish peroxidase (HRP)-mimicking DNAzyme that consists of hemin and G-quadruplex structures, and has been widely applied in colorimetric,[31-36] chemiluminescent[37-39] and electrochemical assays.[40-42] Compared to native HRP, the HRP-mimicking DNAzyme is easier to prepare, cost effective and more stable. More importantly, the HRP-mimicking DNAzyme can be applied to efficiently catalyze the oxidative polymerization of aniline to polyaniline in the presence of $H_2O_2$, which possesses the advantages of easier control over the kinetics of the reaction and high catalysis efficiency.[23,27,43] Furthermore, the HRP-mimicking DNAzyme can be designed ingeniously to rendering

more flexibility to the system. Therefore, introducing DNAzymes with high catalytic activity such as HRP-mimicking DNAzyme to biosensors can not only significantly lower the cost, but also effectively improve the selectivity and enhance the signal response.

Herein, an ultrasensitive SPR biosensing strategy based on HRP-mimicking DNAzyme-catalyzed *in situ* formation of polyaniline for signal amplification has been developed, with bleomycin (BLM) adopted as the proof-of-concept analyte. BLM, a typical antitumor drug, has been widely used in cancer treatment for considerably prolonging life due to its advantages of low myelosuppression and low immunosuppression.[44-47] Thus it is important to develop feasible and reliable methods for ultrasensitive detection of BLM in pharmaceutical and clinical analysis. The in-depth investigation of BLM and DNA interaction has demonstrated that BLM-$Fe^{2+}$ complex can induce the cleavage of DNA strand with specific recognition sequences.[4,48,49] In the present study, a single-stranded DNA (ssDNA) probe (denoted as P1, containing the target recognition sequence) and a G-rich ssDNA reporter (denoted as P2) are ingeniously designed, which partially hybridize to each other and are immobilized on Au disk surface via the S-Au bond between P1 and the gold substrate in the absence of the target BLM. Upon the formation of HRP-mimicking DNAzymes, the catalyzed polyaniline formation occurs, inducing significant SPR angle shift. However, in the presence of BLM, the DNA sequence in P1 is recognized and cleaved by BLM, thus switching off the hybridization between P1 and P2, and subsequently resulting in less HRP-mimicking DNAzymes and little polyaniline on the Au disk surface. As a result, the SPR angle shift is less. Moreover, the amount of SPR angel shift is dependent on the BLM concentration. Therefore, by taking advantage of the polyaniline-assisted SPR signal amplification, ultrasensitive detection of BLM is readily realized using this SPR biosensor. Moreover, this method holds great potential to be adopted as a versatile tool in detecting biomolecules in bioanalysis and clinical biomedicine.

## EXPERIMENTAL SECTION

**Reagents.** The oligonucleotides used in the present study were synthesized and HPLC-purified by Shanghai Sangon Biotechnology Co., Ltd. (China), and the sequences are listed in Table S1 (in Supporting Information). Bleomycin sulfate (BLM) with the contents of A2 and B2 up to 91.6% was purchased from Melone Pharmaceutical Co. Ltd. (Dalian, China). Dactinomycin, mitomycin, and daunorubicin were purchased from Sigma-Aldrich (St. Louis, MO, USA). Aniline monomer (purity 99.5%) was purchased from Tianjin Ruijinte Chemical Co. Ltd. (Tianjin, China). 6-Mercapto-1-hexanol (MCH), hydrochloric acid (HCl), sodium acetate, acetate acid, $NaH_2PO_4$, $Na_2HPO_4$, $NaClO_4$, NaCl and KCl were purchased from Sinopharm Chemical Reagent Co., Ltd. (Shanghai, China), which were of analytical grade and used without further purification or treatment. Human serum samples were obtained from Qingdao Agriculture University Hospital. Ultra-pure water (resistivity > 18.2 MΩ cm @ 25 °C) obtained from a Milli-Q water purification system (Millipore Corp., Bedford, MA, USA) was used throughout the experiments.

**Instrumentation.** SPR measurements were conducted on a Kretschmann-type SPR instrument, SPR Navi 200 (BioNavis, Finland), equipped with a light-emitting diode (LED) at the wavelength of 650 nm as the light source, and a prism with the refraction index of 1.61. A gold-coated glass disk positioned between the flow cell and the prism formed the base of a two-channel sample chamber. Scanning electron microscopy (SEM) images were recorded using a JSM-7500F SEM (JEOL, Japan) with an accelerating voltage of 2.0 kV. All electrochemical measurements were carried out on an Autolab PGSTAT 302N electrochemical analyzer (Metrohm Autolab B.V., the Netherland) at room temperature using a conventional three electrode system: the bare or modified Au electrode was used as the working electrode, an Ag/AgCl electrode as the reference electrode, and a platinum wire as the counter electrode.

**Preparation of MCH/P1/Au.** Before the modification by the capture probe, the SPR Au disk was

cleaned with a cleaning solution containing ammonia and hydrogen peroxide: 1 part of 30% ammonia, 1 part of 30% hydrogen peroxide, and 5 parts of water. First, the cleaning solution was heated to boil, and then the Au disk was placed in it for about 10 minutes. After being removed from the solution, the Au disk was rinsed thoroughly using ultra-pure water for three times, and then dried with nitrogen gas. The cleaned Au disk was immersed into the probe P1 solution (1 μM) at 37 °C for 12 h to allow the thiolated DNA to assemble on its surface, and then followed by rinsing using ultra-pure water. Next the Au disk was subsequently blocked by immersing in 1.0 mM MCH for 90 min, and then thoroughly rinsed with ultra-pure water. The resultant modified disk was denoted as MCH/P1/Au.

**SPR Detection of BLM.** The BLM samples were pretreated by mixing BLM with $Fe^{2+}$ in 1:1 molar ratio to form BLM-$Fe^{2+}$ solution. MCH/P1/Au was immersed into 100 μL of BLM-$Fe^{2+}$ solution and incubated at room temperature for 40 min. Then the as-treated MCH/P1/Au was rinsed thoroughly using ultra-pure water and mounted onto the SPR instrument. After the modified MCH/P1/Au was washed with PBS buffer (100 mM, containing 500 mM NaCl, pH 8.0) to establish a stable baseline, P2 solution (1 μM) was pumped in and hybridized with any uncut P1 probes on the Au disk for 2.0 h, and the resultant Au disk was denoted as P2/MCH/P1/Au. Then PBS (100 mM, pH 7.0) containing 2.0 μM hemin and 300 mM $K^+$ were pumped into the SPR flow cell and incubated with MCH/P1/Au for 1.0 h to form the HRP-mimicking DNAzyme, i.e. hemin/G-quadruplex, and the resultant SPR disk was denoted as Hemin/G4-P2/MCH/P1/Au. Finally, the acetate buffer (100 mM, pH 4.0) containing aniline (30 mM), $H_2O_2$ (5 mM), and hemin (1.0 μM) was pumped into the SPR flow cell and incubated with Hemin/G4-P2/MCH/P1/Au for 3.0 h to initiate the polymerization process, and then the SPR angular reflectivity curves were recorded.

## RESULTS AND DISCUSSION

**Design Principle of the SPR Biosensor.** The working principle of the as-proposed SPR biosensor based on the HRP-mimicking DNAzyme-catalyzed generation of polyaniline to assist signal amplification for ultrasensitive biomolecule detection was illustrated in Scheme 1. In our design, the sequences of two DNA probes, namely P1 and P2, were carefully and rationally designed to partially hybridize with each other, with the dangling G-rich part of P2 being able to form HRP-mimicking DNAzyme, i.e. hemin/G-quadruplex. Probe P1 was first self-assembled on Au disk surface through Au-S bonds and the surface was then blocked with 6-mercapto-1-hexanol (MCH) to form a mixed monolayler to prevent any non-specific adsorption. In the absence of the target analyte (BLM), P1 successfully hybridized with P2 to introduce G-rich DNA sequences on the Au disk surface, which can be induced to fold into the stabilized G4 structure in the presence of $K^+$, successfully forming HRP-mimicking DNAzyme with peroxidase catalytic activity when hemin is efficiently intercalated into the G4 structure. Since the as-generated HRP-mimicking DNAzyme could catalyze the polymerization of aniline to form polyaniline in the presence of $H_2O_2$ and further induced DNA-guided polyaniline deposition, subsequently, polyaniline was successfully fabricated and deposited on the Au disk surface. As a result, a readily amplified SPR signal response was realized, i.e. significant SPR angle shift was observed. However, in the presence of the target analyte (BLM), probe P1 was specifically cleaved *via* the oxidative effect of BLM with Fe (II) as the cofactor, and then due to the cleavage of P1, the residual DNA sequences could not hybridize with P2. Thus, less HRP-mimicking DNAzymes were formed and little polyaniline was deposited on the Au disk surface. As a result, negligible SPR angle shift was observed, as compared to the SPR response in the absence of BLM. Since the amount of polyaniline deposition was dependent on the quantity of HRP-mimicking DNAzyme formed on the SPR disk surface, which was subsequently dependent on the concentration of

BLM, the SPR angle shift of the as-proposed assay was related to the concentration of the target BLM, and ultrasensitive SPR detection of BLM was readily realized.

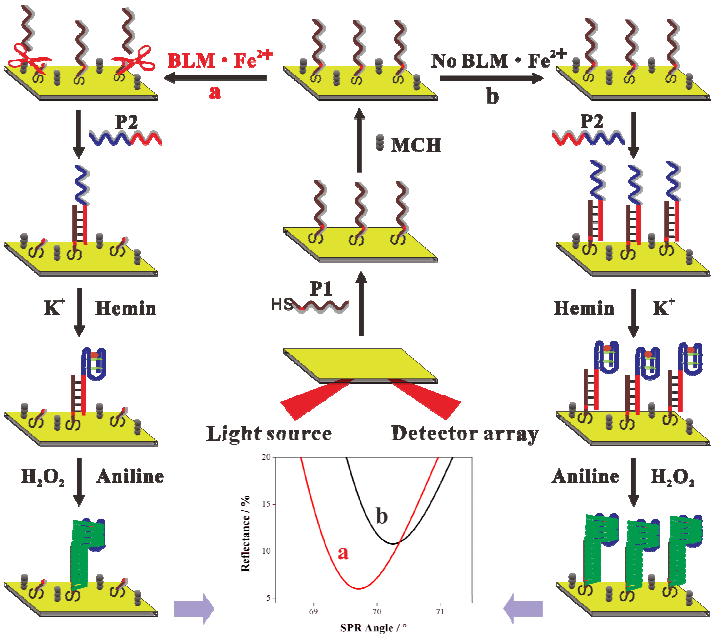


**Scheme 1.** The schematic illustration of the principle of the as-proposed SPR biosensor based on the HRP-mimicking DNAzyme-catalyzed generation of polyaniline to assist signal amplification for ultrasensitive detection of BLM.

**Electrochemical/SPR Characterization of the Biosensor.** The fabrication process of the as-proposed biosensor was first characterized by electrochemical impedance spectroscopy (EIS), and the resulting impedance responses are displayed in Figure 1A. The redox couple of $[K_3Fe(CN)_6]$/$[K_4Fe(CN)_6]$, which is sensitive to the disk surface conditions, was used to demonstrate the electrochemical behaviors of the Au disk at different stages. It was clearly shown that the bare Au disk exhibited a very small semicircle domain with the electron transfer resistance ($R_{et}$) of ~234.7 Ω (curve a in Figure 1A). Nevertheless, after the immobilization of the capture probe P1 on the electrode, a bigger semicircle with $R_{et}$ of ~1105.2 Ω was obtained (curve b in Figure 1A), indicating the anchoring of the thiolated DNA on the electrode surface. MCH treatment produced a further increase of the electron transfer impedance ($R_{et}$, 3886.6 Ω, curve c in

Figure 1A). After the hybridization with G-rich DNA probe P2 and the $K^+$-induced conformation change of the G-rich ssDNA from random-coil to the G4 structure, as compared to MCH/P1/Au, larger negative charge density on electrode surface should be resulted. Thus, it was reasonable to obtain a higher $R_{et}$ value for P2-G4/MCH/P1/Au (curve d in Figure 1A). When hemin was intercalated into the G4 structures, HRP-mimicking DNAzyme was successfully prepared, and the diameter of the semicircle further increased to give an $R_{et}$ of ~5289.6 Ω (curve e in Figure 1A). However, the $R_{et}$ value dramatically decreased once polyaniline was deposited on the Au surface (curve f in Figure 1A), demonstrating the successful deposition of polyaniline on the electrode surface. Undoubtedly, the decrease of $R_{et}$ was attributed to the excellent conductivity of polyaniline, which could largely accelerate the electron transfer of the proposed probe to the electrode surface.

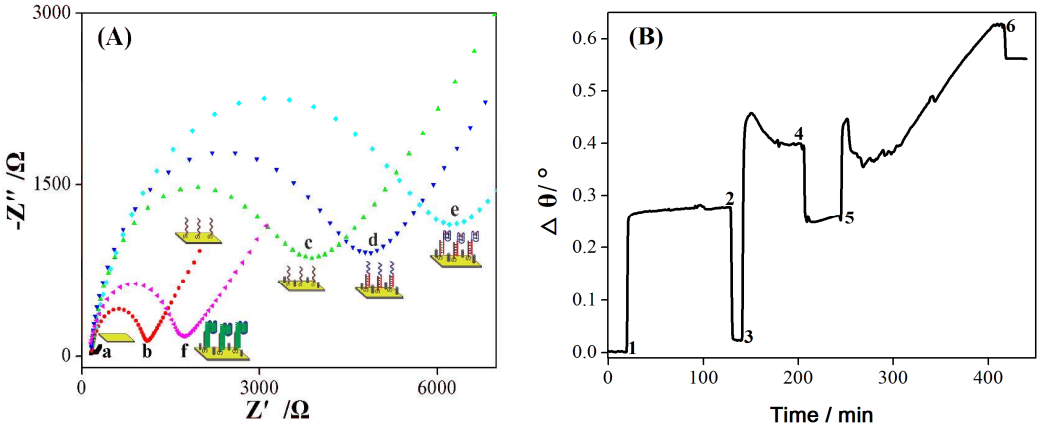


**Figure 1.** (A) Electrochemical impedance spectra (Nyquist plots) of the modified Au electrode at different modification stages: (a) bare Au, (b) P1/Au, (c) MCH/P1/Au, (d) P2/MCH/P1/Au, (e) hemin/P2-G4/MCH/P1/Au, (f) polyaniline/hemin/P2-G4/MCH/P1/Au. These EIS spectra were collected in 0.1 M KCl solution containing $[K_3Fe(CN)_6]/[K_4Fe(CN)_6]$ (5.0 mM, 1:1) mixture. (B) The SPR angle shift ($\Delta\theta$), as compared to that of MCH/P1/Au disk, versus time upon the further modification of SPR disk (MCH/P1/Au) at different stages: (1) pumping in probe P2 solution (1 μM), (2) pumping in PBS buffer, (3) pumping in solution containing $K^+$ (300 mM) and hemin (2.0 μM), (4) pumping in PBS buffer, (5) pumping in solution containing aniline (30 mM) and $H_2O_2$ (5 mM), (6) pumping in PBS buffer; and the concentration of PBS buffer was 10 mM.

The stepwise reactions occurring on the surface of SPR Au disk were also confirmed by SPR measurements. As shown in Figure 1B, with the probe P2 solution being pumped in (stage 1) followed by washing with PBS buffer (stage 2), a small increase of the SPR angel was observed, which was ascribed to the successful hybridization between P1 and P2. Upon the $K^+$-induced conformation change of the G-rich section of P2 and the successful intercalation of hemin into the G4 structure (stages 3 & 4), the SPR angle further shifted, with a $\Delta\theta$ value of 0.25°, indicating the formation of the HRP-mimicking DNAzyme. Moreover, the value of $\Delta\theta$ dramatically increased once polyaniline was deposited on the Au surface (stages 5 & 6), demonstrating the successful deposition of polyaniline on the disk surface. Undoubtedly, the increase of $\Delta\theta$ was attributed to the high refractive index of polyaniline, which could largely increase the light absorption, and thus enhance the SPR responses.

**Feasibility Study of the SPR Biosensor.** To verify the feasibility of the as-proposed sensing strategy, SPR signal upon analyzing the target and those obtained in a series of control experiments were acquired and depicted in Figure 2A. If no polyaniline was formed on the SPR disk, the SPR angle shifted from 69.83° (curve c) to 69.68° (curve b) in the presence of 1 nM BLM, with an angel shift ($\Delta\theta$) of 0.15°. Whereas, if polyanaline was formed on the SPR disk, the SPR angle shifted from 69.72° (curve e) to 70.25° (curve d) upon the addition of 1 nM BLM, with an angel shift ($\Delta\theta$) of 0.53°, which is much more significant than that without polyaniline. It is clearly shown that the target analyte (BLM) indeed caused the SPR angle shift; moreover, the formation of polyaniline on the disk could enhance the SPR angle shift. This is because the formation of a large amount of polyaniline on the SPR Au disk significantly changed the reflectivity of the disk surface, thus resulting in the significant signal amplification effect. However, in the presence of target BLM, BLM-$Fe^{2+}$ specifically cleaved the probe P1, making it impossible for the residual DNA sequences to hybridize with P2. Thus, hemin/G-quadruplex could not be generated on Au disk surface,

and little polyaniline was formed, resulting in a SPR angle similar to that of the blank (curve a). These experimental results clearly demonstrated that polyaniline-assisted signal amplification strategy based on HRP-mimicking DNAzyme catalyzed polyaniline formation can substantially amplify the SPR response and improve the BLM detection sensitivity.

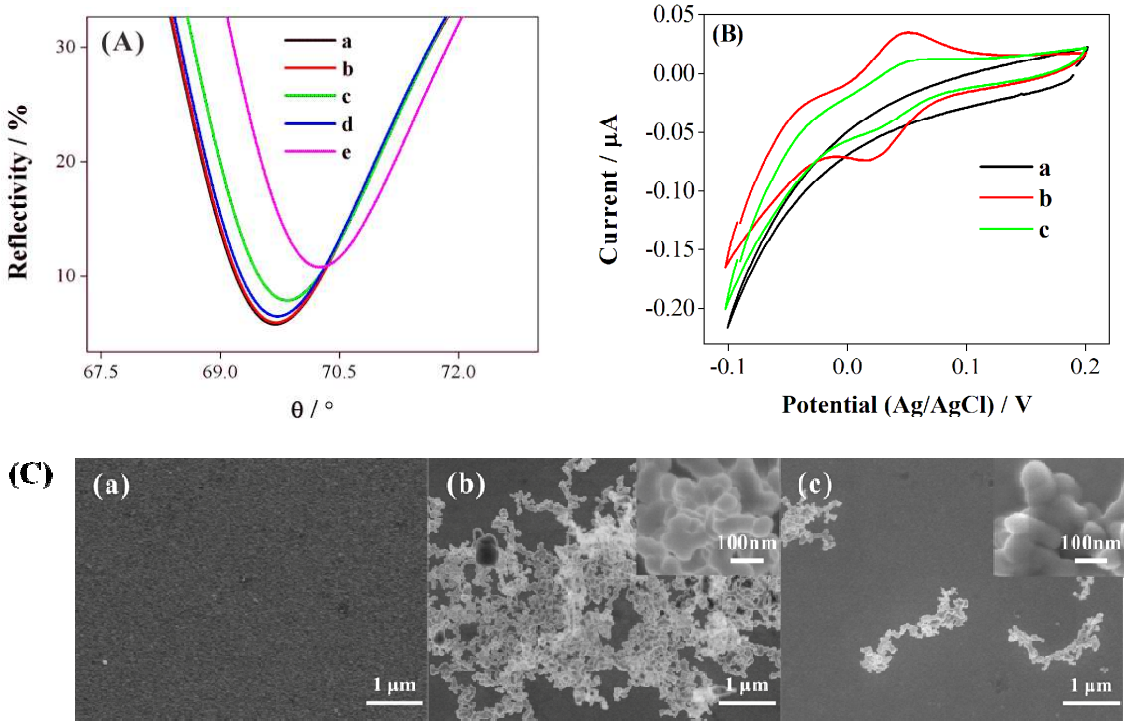


**Figure 2.** (A) SPR angular reflectivity curves under different conditions: (a) bare Au disk; (b) in the presence of 1 nM BLM and without polyaniline formed on Au disk surface; (c) in the absence of BLM and without polyaniline formed on Au disk surface; (d) in the presence of 1 nM BLM and with polyaniline formed on Au disk surface; (e) in the absence of BLM and with polyaniline formed on Au disk surface. (B) Cyclic voltammograms of (a) bare Au electrode, (b) polyaniline/hemin/P2-G4/MCH/P1/Au electrode, and (c) MCH/P1/Au electrode pretreated with BLM (1.0 nM), interacted with P2 and hemin/$K^+$ and then subsequently deposited with polyaniline. (C) Scanning electron microscopy (SEM) images of (a) bare Au disk, (b) polyaniline/hemin/P2-G4/MCH/P1/Au disk, and (c) MCH/P1/Au disk pretreated with BLM (1.0 nM), interacted with P2 and hemin/$K^+$ and then subsequently deposited with polyaniline.

To further verify the feasibility of the proposed sensing strategy, cyclic voltammetric (CV) measurements were carried out. As shown in Figure 2B, compared with the bare Au electrode (curve a), a

pair of well-defined redox peaks were observed for the polyaniline/P2-G4/MCH/P1/Au electrode (curve b), with the anodic and cathodic potentials located at 0.028 V and 0.049 V, respectively. The remarkable redox peaks were undoubtedly attributed to the redox behavior of the polyaniline, which was successfully prepared and deposited on the electrode surface. However, in the presence of 1.0 nM target BLM, the current decreased and the redox peaks became subtle (Figure 2B, curve c), which implied that less polyaniline had been deposited on Au surface, indicating the successful cleavage of probe P1 by BLM-$Fe^{2+}$. This conclusion was also confirmed by the differential pulse voltammetry (DPV) results illustrated in Figure S1 (in Supporting Information). Similarly, low electrochemical signal was observed with BLM present (curve b), and the peak current was about 0.097 μA smaller than that in the absence of BLM sample (curve a). Moreover, SEM results were acquired to further verify the formation of polyaniline on the Au disk surface. As compared to the bare Au surface (Figure 2C-a), nanoparticles with high density were bisible on polyaniline/P2-G4/MCH/P1/Au (Figure 2C-b), indicating the formation of polyaniline on disk surface; whereas, in the presence of 1.0 nM target BLM, nanoparticles with significantly reduced amount were observed (Figure 2C-c), which suggested that probe P1 was successfully cleaved by BLM-$Fe^{2+}$ to result in less polyaniline formed on the Au disk surface.

In this work, the sequences of the DNA probes (P1, and P2) are very important and thus were further investigated. Two DNA probes, namely P1* and P2*, were designed (sequences shown in Table S1 in Supporting Information) and adopted in the as-proposed SPR assay. As compared to P1, P1* did not contain the sequences specific to the BLM-$Fe^{2+}$ cleavage; as compared to P2, P2* did not contain the G-rich sequences. As demonstrated in Figure S2 (in Supporting Information), with P1 substituted by P1*, hardly any $\Delta\theta$ value change was detected whether BLM present or not, and similarly, with P2 substituted by P2*, no obvious $\Delta\theta$ value change was observed whether BLM present or not. Therefore, these results

justified the design of the sequences for P1 and P2.

**Optimization of Experimental Conditions for BLM Detection.** In the BLM analysis, the formation of polyaniline is essential for SPR signal amplification. To achieve the best performance for BLM analysis, the polyaniline formation conditions were systematically investigated. First, to investigate the effect of pH, the SPR measurements were conducted upon the incubation of hemin/P2-G4/MCH/P1/Au with $H_2O_2$ and aniline under different pH values ranging from 2 to 8. As shown in Figure S3A (in Supporting Information), the SPR angle shift ($\Delta\theta$) increased as pH increased from 2 to 4.3. With pH further increased, $\Delta\theta$ decreased obviously. Thus 4.3 was chosen as the optimum pH value, which was in accordance with the previously reported work.[26] Next, the polymerization reaction time for polyaniline formation was studied. As shown in Figure S3B (in Supporting Information), the SPR angle shift ($\Delta\theta$) elevated at a fast rate in the initial stage and the increase slowed down after 180 min. Therefore, 180 min was selected as the optimal reaction time. Finally, the concentrations of aniline and $H_2O_2$ were also investigated, respectively. As shown in Figure S3C (in Supporting Information), with the concentration of aniline increased from 1 to 60 mM, $\Delta\theta$ initially increased and leveled off after the aniline concentration reached 30 mM. Thus, 30 mM was chosen as the optimum aniline concentration. Similarly, based on Figure 3SD (in Supporting Information), 5 mM was chosen as the optimum concentration for $H_2O_2$. .

**Analytical Performance of the SPR Biosensor.** The aforementioned feasibility study results of the as-proposed SPR biosensor suggested that polyaniline-assisted signal amplification strategy could be utilized for the amplified biomolecule detection with improved sensitivity. We challenged this SPR biosensor by detecting target BLM with different concentrations to test its analytical performance under the optimal experimental conditions. Figure 3A illustrates the SPR response observed in the presence of BLM with different concentrations. It is clearly shown that, as compared to that of the blank (MCH/P1/Au), the

SPR angle shift decreased significantly with the elevated concentration of target BLM, which could be attributed to the fact that the presence of more target BLM caused the generation of less HRP-mimicking DNAzyme and reduced polyaniline formation, thus reducing the SPR angle shift. A calibration curve made by plotting $\Delta\theta$ ($\Delta\theta=\theta_1-\theta_0$, in which $\theta_0$ is the SPR angle of MCH/P1/Au, i.e. the blank; $\theta_1$ is the SPR angle of Hemin/G4-P2/MCH/P1/Au in the presence of BLM with different concentrations) *vs.* the BLM concentration is shown in Figure 3B. It can be clearly seen that $\Delta\theta$ was linearly proportional to the BLM concentration ranging from 0.001 to 0.1 nM. The resulting linear regression equation was obtained as $\Delta\theta = -3.74C_{BLM} + 0.54$ ($\Delta\theta$ in the units of °, and $C_{BLM}$ in the units of nM), with the correlation coefficient of $R^2=0.9962$. Additionally, the detection limit was determined to be 0.35 pM (based on 3σ), which, as shown in Table S2 (in Supporting Information), was much lower than that of the existing sensing strategies for BLM quantification, such as DNAzyme catalyzed cyclic cleavage of DNA hairpin probe, colorimetry，electrochemistry and so on.[48-51] These results demonstrated the SPR signal amplification efficiency of the polyaniline-assisted strategy and revealed that ultrasensitive detection of BLM was indeed realized by the as-proposed SPR biosensor.

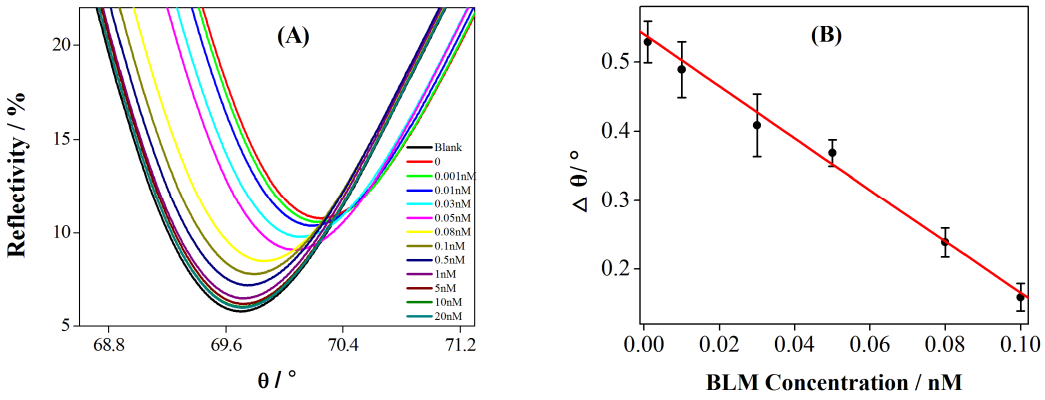


**Figure 3.** (A) SPR angular reflectivity curves corresponding to the analysis of target BLM with different concentrations (ranging from 0 to 20 nM); (B) Linear relationship between $\Delta\theta$ and the BLM concentration ranging from 0.001 to 0.1 nM. The error bars represent the standard deviation of three repetitive measurements.

**Selectivity of the SPR Biosensor.** To investigate the selectivity and specificity of the as-proposed SPR biosensor, we performed several contrast experiments by using three other target analogies as the interfering substances, namely, daunorubincin, mitomycin, and dactinomycin. As shown in Figure 4, the system showed small SPR angle shift only in the presence of BLM. Nevertheless, in the presence of one of the three other interfering substances, the SPR response exhibited no obvious change compared with that of the blank. Moreover, a 0.1 nM BLM sample containing daunorubincin, mitomycin, and dactinomycin exhibited no obvious SPR angle changes compared with that obtained from 0.1 nM BLM only. Thus, the as-proposed SPR biosensor exhibited good performance for discriminating BLM against other interfering drugs.

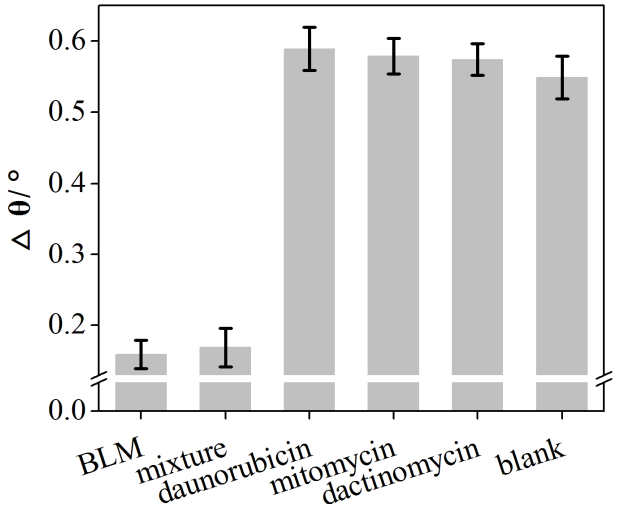


**Figure 4.** Comparison of the SPR angle shifts in the presence of BLM, daunorubincin, mitomycin, dactinomycin, and the mixture containing BLM, daunorubicin, mitomycin and dactinomycin, respectively, in which " blank " indicates the condition: in the absence of BLM. The concentrations of all analytes were 0.1 nM. The error bars represent the standard deviation of three repetitive measurements.

**Real Sample Analysis.** In order to test the applicability of the as-proposed assay of BLM in clinical samples, recovery experiments were carried out by spiking BLM-$Fe^{2+}$ with different concentrations into human serum samples. In the mixed solution, the volume proportion of serum was 50%. As clearly shown

in Table 1, for BLM with different concentrations of 0.0050 nM, 0.0300 nM and 0.0700 nM, there was good agreement between the added and the measured values of BLM concentrations, and the recoveries were found to be in the range of 98% to 103%, suggesting no severe interferences in such samples. Moreover, the relative standard deviations (*RSD*) of three repetitive measurements for these samples were all below 3.3%, demonstrating good reproducibility. These results indicated that the as-proposed SPR biosensor had good reliability and reproducibility, and could be successfully applied for the detection of BLM in clinical samples.

**Table 1.** Detection of BLM spiked in serum samples (n = 3)

| Sample No. | Added (nM) | Mean measured (nM) | Mean recovery [a] (%) | RSD (%) |
|---|---|---|---|---|
| 1 | 0.0050 | 0.0052 | 103 | 3.24 |
| 2 | 0.0300 | 0.0295 | 98 | 2.85 |
| 3 | 0.0700 | 0.0718 | 103 | 2.97 |

[a]Recovery (%) = $100 \times (c_{\text{mean measured}} / c_{\text{added}})$

## CONCLUSIONS

In this work an SPR biosensor has been designed for ultrasensitive BLM detection based on the HRP-mimicking DNAzyme catalyzed *in situ* formation of polyaniline and polyaniline-assisted SPR signal amplification strategy. The HRP-mimicking DNAzyme, i.e. hemin/G-quadruplex, with the advantages of simple and convenient fabrication route, stability, and reproducibility, acts as an efficient catalyst for the oxidative polymerization of aniline to polyaniline and its subsequent deposition on the DNA structures. Thus, owing to the high refractive index of polyaniline, significantly enhanced SPR response is realized. With BLM adopted as a proof-of-concept target, the as-proposed biosensor exhibits ultrahigh sensitivity for BLM detection, and a detection limit down to 0.35 pM is obtained, which is much lower than that of previously reported BLM biosensors. The applicability of this SPR biosensor for real sample analysis has

also been demonstrated by detecting BLM spiked in human serum samples. Moreover, ultrasensitive SPR detection of other biomolecules can be readily realized by simply changing the specific target recognition DNA sequences, thus providing a versatile SPR biosensing platform for ultrasensitive detection of a variety of analytes. Therefore, the as-proposed SPR biosensor has great potential to be applied in the areas of bioanalysis and clinical biomedicine.

## Notes

The authors declare no competing financial interest.

## ACKNOWLEDGEMENTS

This work was funded by the National Natural Science Foundation of China (Nos. 21575074, 21375072 and 21605093), the Basic Research Program of Qingdao (No. 14-2-4-102-jch), the Research Foundation for Distinguished Scholars of Qingdao Agricultural University (No. 663-1113334), the Project of Shandong Province Higher Educational Science and Technology Program (No. J15LC08), and the Special Foundation for Taishan Scholar of Shandong Province.

## REFERENCES


(1) Kobayashi, H.; Ogawa, M.; Alford, R.; Choyke, P. L.; Urano, Y. *Chem. Rev*. **2010**, 110, 2620–2640.

(2) Beija, M.; Afonso, C. A. M.; Martnho, J. M. G. *Chem. Soc. Rev.* **2009**, 38, 2410–2433.

(3) Li, F.; Feng, Y.; Zhao, C.; Tang, B. *Chem. Commun.* **2011**, 47, 11909–11911.

(4) Li, F.; Feng, Y.; Zhao, C.; Li, P.; Tang, B. *Chem. Commun*. **2012**, 48, 127–129.

(5) Hou, T.; Zhang, L. F.; Sun, X. Z.; Li, F. *Biosens. Bioelectron.* **2016,** *75*, 359-364.

(6) Li, L.; Liu, H.; Shen, Y.; Zhang, J.; Zhu, J. J. *Anal. Chem*. **2011**, 83, 661–665.

(7) Chen, Z.; Zu, Y. *J. Phys. Chem. C*. **2009**, 113, 21877–21882.

(8) Huang, C. F.; Yao, G. H.; Liang, R.P.; Qiu, J. D. *Biosens. Bioelectron*. **2013**, 50, 305–310.

(9) Liu, Y.; Young, M. C.; Moshe, O.; Cheng, Q.; Hooley, R. J. *Angew. Chem. Int. Ed*. **2012**, 51, 7748–7751.

(10) Kanoh, N.; Kyo, M.; Inamori, K.; Ando, A.; Asami, A.; Nakao, A.; Osada, H. *Anal. Chem*. **2006**, 78, 2226–2230.

(11) Wang, J.; Zhou, H. S. *Anal. Chem.* **2008**, 80, 7174–7178.

(12) Xue, T.; Cui, X.; Guan, W.; Wang, Q.; Liu, C.; Wang, H. Qi, K.;Singh, D. J.; Zheng, W. *Biosens. Bioelectron.* **2014**, 58, 374–379.

(13) Pelossof, G.; Vered, R. T.; Willner, I. *Anal. Chem*. **2012**, 84, 3703–3709.

(14) Yao, G. H.; Liang, R. P.; Yu, X. D.; Huang, C. F.; Zhang, L.; Qiu, J. D. *Anal. Chem*. **2015**, 87, 929–936.

(15) Xue, T.; Cui, X.; Chen, J.; Liu, C.; Wang, Q.; Wang, H.; Zheng, W. *ACS Appl. Mater. Interfaces*. **2013**, 5, 2096–2103.

(16) Roy, S.; Dixit, C. K.; Manickam, G.; Daniels, S.; Mcdonagh, C. *Langmuir* **2013**, 29, 4430–4433.

(17) Huang, S.; He, Q.; Xu, S.; Wang, L. *Anal. Chem*. **2015**, 87, 5451–5456.

(18) Li, F.; Yang, L.; Chen, M.; Qian, Y.; Tang, B. *Biosens. Bioelectron*. **2013**, 41, 903–906.

(19) Wang, Z.; Liu, S.; Wu, P.; Cai, C. *Anal.Chem*. **2009**, 81, 1638–1645.

(20) Mccoy, C. H.; Lorkovic, I. M.; Wrighton, M.S. *J. Am. Chem. Soc*. **1995**, 117, 6934–6943.

(21) Yue, J.; Epstein, A. J. *J. Am. Chem.Soc*. **1990**, 112, 2800–2801.

(22) Prathap, M. U. A.; Chaurasia, A. K.; Sawant, S. N.; Apte, S. K. *Anal.Chem*.**2012**, 84, 6672–6678.

(23) Liu, Y.; Wei, M.; Liu, X.; Wei, W.; Zhao, H.; Zhang, Y.; Liu, S. *Chem. Commun.* **2016,** 52, 1796–1799.

(24) Raitman, O. A.; Katz, E.; Buckmann, A. F.; Willner, I. *J. Am. Chem. Soc.* **2002**, 124, 6487–6496.

(25) Huang, J.; Virji, S.; Weiller, B. H.; Kaner, R. B. *J. Am. Chem. Soc*. **2003**, 125, 314–315.

(26) Gao, Z. Q.; Rafea, S.; Lim, L. H. *Adv. Mater.* **2007**, 19, 602–606.

(27) Li, F.; Yang, L. M.; Chen, M. Q.; Qian, Y.; Tang, B. *Biosens. Bioelectron.* **2013**, 41, 903–906.

(28) Su, X. D.; Teh, H. F.; Aung, K. M. M.; Zong, Y.; Gao, Z. Q. *Biosens. Bioelectron.* **2008**, 23, 1715–1720

(29) Wang, F.; Lu, C. H.; Willner, I. *Chem. Rev*. **2014**, 114, 2881–2941.

(30) Liu, X.; Lu, C. H.; Willner, I. *Acc. Chem. Res*. **2014**, 47, 1673–1680.

(31) Elbaz, J.; Moshe, M.; Shlyahovsky, B.; Willner, I. *Chem.–Eur. J.* **2009**, 15, 3411–3418.

(32) Zhou, W.; Gong, X.; Xiang, Y.; Yuan, R.; Chai, Y. *Anal. Chem.* **2014**, 86, 953–958.

(33) Li, H.; Wu, Z.; Qiu, L.; Liu, J.; Wang, C.; Shen, G.; Yu, R. *Biosens. Bioelectron*. **2013**, 50, 180–185.

(34) Wang, F.; Lu, C.-H.; Liu, X.; Freage, L.; Willner, I. *Anal. Chem.* **2014**, 86, 1614–1621.

(35) Sun, H.; Li, X.; Li, Y.; Fan, L.; Kraatz, H.-B. *Analyst.* **2013**, 138, 856–862.

(36) Huang, Y.; Chen, J.; Zhao, S. L.; Shi, M.; Chen, Z. F.; Liang, H. *Anal. Chem*. **2013**, 85, 4423–4430.

(37) Freeman, R.; Liu, X.; Willner, I. *J. Am. Chem. Soc.* **2011**, 133, 11597–11604.

(38) Gao, Y.; Li, B. *Anal. Chem.* **2013**, 85, 11494–11500.

(39) Liu, X.; Freeman, R.; Golub, E.; Willner, I. *ACS Nano.* **2011**, 5, 7648−7655.

(40) Liu, S.; Wang, C.; Zhang, C.; Wang, Y.; Tang, B. *Anal. Chem.* **2013**, 85, 2282−2288.

(41) Wang, G.; He, X.; Chen, L.; Zhu, Y.; Zhang, X.; Wang, L. *Biosens. Bioelectron.* **2013**, 50, 210−216.

(42) Wang, X.; Ding, Z.; Ren, Q.; Qin, W. *Anal. Chem.* **2013**, 85, 1945−1950.

(43) Zhang, L.; Wei, M.; Gao, C.; Wei, W.; Zhang, Y.; Liu, S. *Biosens. Bioelectron.* **2015**, 73, 188−194.

(44) Galm, U.; Hager, M. H.; Van Lanen, S. G.; Ju, J.; Thorson, J. S.; Shen, B. *Chem. Rev.* **2005**, 105, 739–758.

(45) Yu, Z. Q.; Schmaltz, R. M.; Bozeman, T. C.; Paul, R.; Rishel, M. J.; Tsosie, K. S.; Hecht, S. M. *J. Am. Chem. Soc*. **2013**, 135, 2883–2886.

(46) Akiyama, Y.; Ma, Q.; Edgar, E.; Laikhter, A.; Hecht, S. M. *J. Am. Chem. Soc.* **2008**, 130, 9650–9651.

(47) Giroux, R. A.; Hecht, S. M. *J. Am. Chem. Soc.* **2010**, 132, 16987–16996.

(48) Gao, F, L.; Lei, J, P.; Ju, H, X. *Chem. Commun*. **2013**, 49, 7561–7563.

(49) Yin, B, C.; Wu, D.; Ye, B, C. *Anal. Chem*. **2010**, 82, 8272–8277.

(50) Li, F.; Feng, Y.; Zhao, C.; Tang, B. Biosens. Bioelectron. **2011**, 26,4628–4631.

(51) Chang, Y.; Zhang, P.; Yu, Y.; Du, Y, Q, Wang, W.; Huang, C, Z. *Analytical Methods,* **2013**, 5, 6200–6204.

**For TOC only**

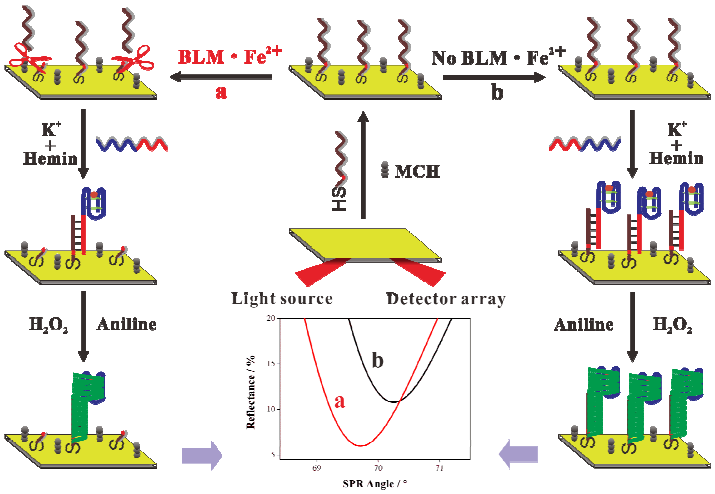
BLM • Fe2+
a
No BLM • Fe2+
b
K+
+
Hemin
MCH
HS
Light source
Detector array
H2O2
Aniline
Aniline
H2O2
K+
+
Hemin
Reflectance / %
SPR Angle / °
a
b